Radio Synchrotron Emission from a Bow Shock Around the Gas Cloud G2 Heading Toward the Galactic Center

The Astrophysical Journal Letters, 757:L20 (5pp), 2012 October 1 doi:10.1088/2041-8205/757/2/L20

RADIO SYNCHROTRON EMISSION FROM A BOW SHOCK AROUND THE GAS CLOUD G2 HEADING TOWARD THE GALACTIC CENTER

Ramesh Narayan[1], Feryal Özel[2], and Lorenzo Sironi[1,3]
[1] Harvard-Smithsonian Center for Astrophysics, 60 Garden St., Cambridge, MA 02138, USA
[2] Department of Astronomy, University of Arizona, 933 N. Cherry Ave., Tucson, AZ 85721, USA
Received 2012 July 17; accepted 2012 August 13; published 2012 September 7

ABSTRACT

A dense ionized cloud of gas has been recently discovered to be moving directly toward the supermassive black hole, Sgr A*, at the Galactic center. In 2013 June, at the pericenter of its highly eccentric orbit, the cloud will be approximately 3100 Schwarzschild radii from the black hole and will move supersonically through the ambient hot gas with a velocity of $v_p \approx 5400$ km s^{-1}. A bow shock is likely to form in front of the cloud and could accelerate electrons to relativistic energies. We estimate via particle-in-cell simulations the energy distribution of the accelerated electrons and show that the non-thermal synchrotron emission from these electrons might exceed the quiescent radio emission from Sgr A* by a factor of several. The enhanced radio emission should be detectable at GHz and higher frequencies around the time of pericentric passage and in the following months. The bow shock emission is expected to be displaced from the quiescent radio emission of Sgr A* by ∼33 mas. Interferometric observations could resolve potential changes in the radio image of Sgr A* at wavelengths $\lesssim$6 cm.

Key words: accretion, accretion disks – black hole physics – galaxies: active – Galaxy: center

Online-only material: color figures

1. INTRODUCTION

Recent submillimeter observations revealed a dense ionized cloud of gas known as G2, rapidly approaching Sgr A*, the black hole at the Galactic center (Gillessen et al. 2012). The cloud is on a highly eccentric trajectory, with a 2011 distance from the black hole of 1.8×10^{16} cm. The pericentric passage, which is expected to occur in mid 2013, will bring the cloud within 4×10^{15} cm of the supermassive black hole. Given the mass of the black hole, which is determined through observations of nearby stellar orbits to be $M = 4.3 \times 10^6\ M_\odot$ (Ghez et al. 2008; Gillessen et al. 2009), this pericentric distance is only $R_p = 3100\,R_S$, where the Schwarzschild radius $R_S = 1.27 \times 10^{12}$ cm.

The accretion flow around the black hole extends to the Bondi radius $\sim10^5 R_S$ (e.g., Yuan et al. 2003) and powers the multiwavelength emission observed from it. The flux at 1 GHz is $\simeq$0.5 Jy, rising to $\approx$4 Jy at 500 GHz, before rapidly declining at higher frequencies. The radio emission has been successfully modeled as synchrotron radiation from relativistic electrons, either in a radiatively inefficient accretion flow (ADAF; Narayan et al. 1995; Özel et al. 2000) or in a jet (Falcke & Markoff 2000). At the lowest end of the spectrum—$\nu \sim$ 1–10 GHz—the radio emission shows flux variability on a timescale of months to years with a root mean square amplitude ∼10% (Zhao et al. 1989; Falcke 1999; Macquart & Bower 2006).

At its pericentric passage, the gas cloud will interact with the accretion flow, and this may significantly change its dynamics. Here, we show that a bow shock is likely to develop as the cloud plows through the hot, tenuous plasma at R_p. In Section 2 we calculate the properties of the bow shock, and in Section 3 we estimate the energy distribution of electrons accelerated at this shock. In Section 4, we calculate the extra radio emission that will result from these accelerated electrons. For likely electron energy distributions, the additional emission is ∼10 Jy at frequencies ∼1–10 GHz. This is well above the quiescent emission from Sgr A* and should be easily detectable. We also show that the flux increase will be accompanied by significant changes in the spectral index. In Section 5, we summarize our findings and argue that interferometric observations could resolve potential changes in the radio image of Sgr A* caused by the interaction of the cloud with the accretion flow.

2. THE BOW SHOCK AROUND G2 AT PERICENTER

We first calculate the dynamics of the interaction of the cloud G2 with the accretion flow around the black hole. Since the orbit of G2 is highly eccentric, its velocity at pericenter will be

$$v_p \approx \left(\frac{2GM}{R_p}\right)^{1/2} = 5400\ \mathrm{km\,s^{-1}}. \quad (1)$$

The properties of the ambient gas at the pericentric distance R_p can be obtained from ADAF models of Sgr A*. Within that context and using Yuan et al. (2003) and Xu et al. (2006) as a guide, Gillessen et al. (2012) estimated the gas density and temperature at $R = R_p$ to be[4]

$$n \approx 930\left(\frac{1.4\times10^4\ R_S}{R_p}\right)\ \mathrm{cm^{-3}} = 4200\,\mathrm{cm^{-3}}, \quad T \approx 10^9\ \mathrm{K}. \quad (2)$$

To estimate the sound speed, we use the fact that the gas in the ADAF is likely to have its Bernoulli parameter close to zero (Narayan & Yi 1994). Thus,

$$Be = -\frac{GM}{R_p} + \frac{1}{2}v_R^2 + \frac{1}{2}v_\phi^2 + w \approx 0, \quad (3)$$

where $w = \Gamma p/(\Gamma-1)\rho$ is the enthalpy per unit mass, $\Gamma = 5/3$ is the adiabatic index, p is the pressure, and ρ the density of

[3] NASA Einstein Post-Doctoral Fellow.

[4] Some models suggest a temperature closer to $10^{8.5}$ K, but this small uncertainty is not important for what follows.

the gas. Because the radial velocity v_R is small compared to the azimuthal velocity v_ϕ, we ignore it. We also assume that v_ϕ^2 is roughly half the Keplerian value, which is appropriate for an ADAF. Under these assumptions, we estimate the adiabatic sound speed of the gas, $c_{\rm ad} = \sqrt{\Gamma p/\rho}$, to be

$$c_{\rm ad} \approx v_p/2 \approx 2700 \ {\rm km\ s^{-1}}. \quad (4)$$

The gas pressure is then given by

$$p = \frac{1}{\Gamma}\rho c_{\rm ad}^2 \approx 3.1 \times 10^{-4} \ {\rm erg\ cm^{-3}}. \quad (5)$$

Finally, if we assume that the magnetic pressure is about 10% of the gas pressure, as is typical in an ADAF, we then estimate the magnetic field strength in the ambient gas to be ≈0.03 G.

There is currently no information on the relative orientation of the orbits of G2 and the ambient gas in the accretion flow. However, because the velocity v_p of the cloud at pericenter is substantially larger than the local gas velocity v_ϕ, we expect the relative velocity at R_p to be dominated by v_p. Thus, G2 will move with a Mach number $\mathcal{M} \approx 2$ near pericenter. Using Rankine–Hugoniot jump conditions for a non-relativistic shock, we estimate for the shocked gas:

$$\frac{n_{\rm shock}}{n} = \frac{(\Gamma+1)\mathcal{M}^2}{(\Gamma-1)\mathcal{M}^2+2} \approx 2.3, \quad (6)$$

$$\frac{p_{\rm shock}}{p} = \frac{(\Gamma+1)+2\Gamma(\mathcal{M}^2-1)}{(\Gamma+1)} \approx 4.8. \quad (7)$$

For a Mach number $\mathcal{M} \approx 2$, the magnetic field strength will be roughly doubled by compression in the shock, i.e., $B_{\rm shock} \approx 0.06$ G. Similarly, the post-shock temperature will be a factor of a few larger than the temperature of the pre-shock gas. Thus, the mean thermal energy of the shocked electrons should be close to $m_e c^2$, i.e., the electrons will be quasi-relativistic.

Gillessen et al. (2012) estimated the equivalent spherical size of the cloud in 2011 to be 15 mas, which corresponds to a physical radius of 1.9×10^{15} cm. As the cloud approaches the pericenter along its highly eccentric orbit, it is expected to be tidally stretched (Gillessen et al. 2012; Burkert et al. 2012), primarily along the direction of motion. We estimate the cross-sectional area A of the bow shock using the frontal size of the cloud, which will remain approximately constant at $\pi(10^{15}\ {\rm cm})^2$.

Figure 1 shows the Mach number of G2's motion through the ambient medium (assuming that the medium is at rest) and the temperature of the medium as a function of time. A bow shock will form when $\mathcal{M}$ exceeds unity, which is expected to last for about a year around pericenter. The temperature of the medium, which has a significant effect on particle acceleration (see Section 3), is also strongly peaked around pericenter. Taking the relative velocity between G2 and the ambient medium to be equal to v_p, and conservatively taking the duration of the bow shock to be six months, we estimate the total number of shocked electrons to be

$$N_{\rm shock} \approx A\ v_p\ t_p\ n = 1.1 \times 10^{50}. \quad (8)$$

3. ACCELERATION OF ELECTRONS IN THE BOW SHOCK

A variety of astrophysical evidence suggests that particles are accelerated efficiently via the Fermi and shock-drift acceleration mechanisms in shocks (e.g., Blandford & Eichler 1987).

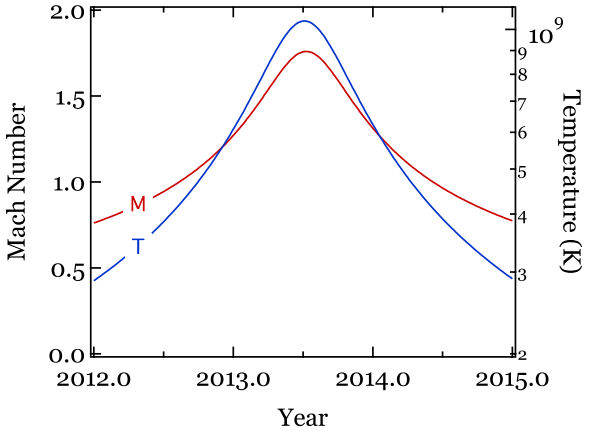

Figure 1. Mach number $\mathcal{M}$ of G2's motion through the hot accretion flow around Sgr A* and temperature T of this medium as a function of time. Pericentric passage occurs in year 2013.5. Both $\mathcal{M}$ and T peak sharply around pericenter, and a bow shock should be present for approximately 6 months on either side of pericenter. Since the orientation of the angular momentum vector of the accreting gas is not known, for simplicity the gas has been assumed to be at rest.

(A color version of this figure is available in the online journal.)

Typically, these processes give rise to a non-thermal power-law tail in the energy distribution of the particles. The parameters of the bow shock of G2 correspond to an interesting regime that has not been well studied. The shock is non-relativistic, but the upstream electrons are quasi-relativistic ($kT_e \lesssim m_e c^2$). In addition, the shock has a modest Mach number $\mathcal{M} \approx 2$, and the upstream gas is fairly strongly magnetized, corresponding to an Alfvénic Mach number $\mathcal{M}_A \approx 8$.

We studied the acceleration of electrons in the bow shock of G2 by means of two-dimensional first-principles numerical simulations, with the particle-in-cell (PIC) code TRISTAN-MP (Spitkovsky 2005). The simulation setup parallels very closely the one employed by Riquelme & Spitkovsky (2011), with the magnetic field lying initially in the simulation plane, oriented at an oblique angle with respect to the flow velocity. For computational convenience, we chose a reduced mass ratio $m_p/m_e = 100$, but we tested that our results remain the same for larger mass ratios, when all the physical quantities are scaled appropriately. Specifically, we ran simulations spanning the range $m_p/m_e = 25$–400, fixing the electron temperature (equal to the proton temperature) and the shock sonic and Alfvénic Mach numbers, and we measured the time in units of the inverse proton cyclotron frequency $\omega_{\rm ci}^{-1}$. We also checked the convergence of our results with respect to the spatial resolution and the number of computational particles per cell.

We find that at the shock, a fraction of the incoming electrons are reflected backward by the shock-compressed magnetic field (Matsukiyo et al. 2011) or by scattering off of electron whistler waves excited in the shock transition layer (Riquelme & Spitkovsky 2011). For quasi-relativistic electron temperatures, the reflected electrons are fast enough to remain ahead of the shock, resisting advection downstream by the oblique pre-shock field. While the electrons gyrate around the shock, they are energized by shock-drift acceleration (e.g., Begelman & Kirk 1990) and form a local non-thermal population, just upstream of the shock.

The temporal evolution of this population is shown in the left panel of Figure 2, for parameters relevant to the bow shock of G2: $T_p = T_e = 10^9$ K $\simeq 0.2\, m_e c^2/k$, $\mathcal{M} = 2$ and $\mathcal{M}_A = 8$. At late times, the shock-accelerated electrons populate a power-law tail with a slope of $p = 2.2$ beyond an electron Lorentz factor

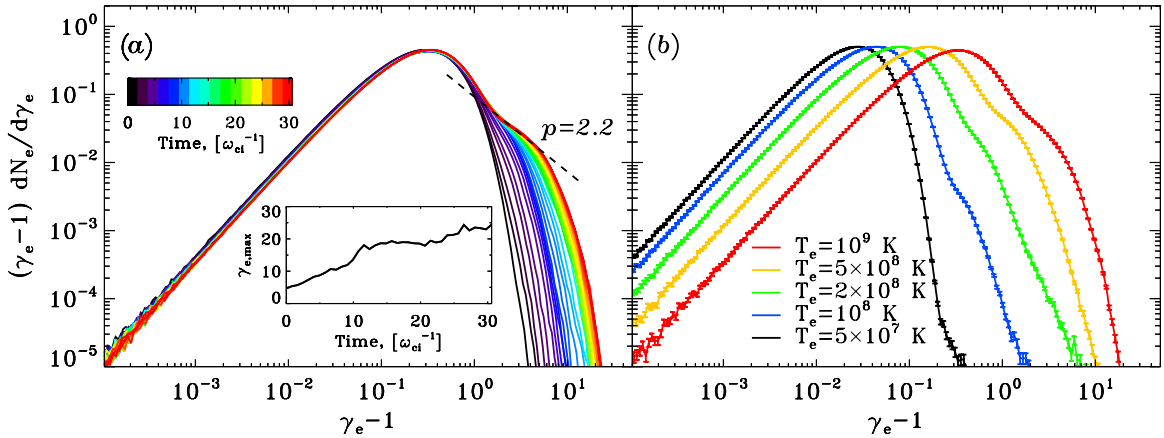

Figure 2. Electron energy spectrum just upstream of the shock, normalized to the pre-shock electron density. (Left) The temporal evolution of the spectrum, for $T_e = 10^9$ K, $\mathcal{M} = 2$ and $\mathcal{M}_A = 8$. With time, the non-thermal component approaches a power-law tail with index $p = 2.2$ (dashed line) and its cutoff energy steadily increases (inset). (Right) Electron energy spectrum at $\omega_{ci}t = 14$ for different upstream temperatures (therefore, different $\mathcal{M}$), with fixed $\mathcal{M}_A = 8$ and fixed flow velocity. The regime $10^{8.5}\text{K} \lesssim T_e \lesssim 10^9$ K is relevant for the accretion flow around Sgr A* at a distance R_p from the black hole.

$\gamma_e \simeq 2$, containing roughly 5% of the incoming electrons. The upper energy cutoff of the electron spectrum steadily increases with time, as shown in the left-panel inset of Figure 2, suggesting that the distribution will asymptote at late times to a power law with $p \lesssim 2.2$ extending to very large values of γ_e. The counter streaming between the incoming flow and the shock-reflected electrons triggers the Weibel filamentation instability ahead of the shock (Weibel 1959; Medvedev & Loeb 1999), with the wavevector perpendicular to the pre-shock field.[5] By scattering off of the magnetic field generated by the Weibel instability, the shock-reflected electrons are deflected back toward the shock, participating in a Fermi-like acceleration process. In the downstream region, they populate a power-law tail of similar normalization and slope as the pre-shock spectrum shown in the left panel of Figure 2.

The distribution of non-thermal electrons is sensitive to the electron temperature ahead of the shock. As shown in the right panel of Figure 2, the normalization of the power-law tail is reduced by almost one order of magnitude when the electron temperature decreases from $T_e = 10^9$ K (red curve) down to $T_e = 10^8$ K (blue curve), with the flow velocity staying fixed. If the upstream plasma is colder, fewer electrons are reflected back at the shock (Matsukiyo et al. 2011), so a smaller fraction of the incoming electrons are injected in the shock-drift acceleration process. In the limit of cold upstream plasmas studied by Riquelme & Spitkovsky (2011), electrons are not efficiently reflected back from the shock (black curve in Figure 2, for $T_e = 5 \times 10^7$ K). In this case, the process of Weibel-mediated acceleration described above does not operate and the resulting downstream non-thermal tail becomes steeper, with $p \gtrsim 3$ (Riquelme & Spitkovsky 2011).

The acceleration efficiency of 5% and the power-law index of 2.2 that we find for the parameters of the bow shock of G2, combined with our estimate for the total number of shocked electrons given in Equation (8), allows us to write the electron energy distribution as

$$\frac{dN}{d\gamma_e} \approx 2 \times 10^{49}\, \gamma_e^{-2.2}, \quad \gamma_e \geqslant 2. \tag{9}$$

[5] We point out that the Weibel mode can only be captured by means of multi-dimensional simulations and was, therefore, absent in the one-dimensional experiments of Matsukiyo et al. (2011).

In the next section, we calculate the properties of the synchrotron emission that arises from this electron distribution.

4. EXPECTATIONS FOR NON-THERMAL SYNCHROTRON EMISSION

The peak of the synchrotron emission from an electron with a Lorentz factor γ_e occurs at a frequency

$$\nu = \frac{3}{4\pi}\gamma_e^2 \frac{eB}{m_e c}, \text{ i.e., } \nu_{\rm GHz} \equiv \frac{\nu}{10^9\ \text{Hz}}$$
$$\approx 2.4 \times 10^{-4} \left(\frac{B}{0.06\ \text{G}}\right) \gamma_e^2, \tag{10}$$

where we have scaled the result to the expected field strength of 0.06 G in the shocked medium. Conversely, we can invert the above relation to infer the Lorentz factor of the electrons that contribute predominantly to the emission at a particular frequency:

$$\gamma_e \approx 65 \left(\frac{B}{0.06\ \text{G}}\right)^{-1/2} \nu_{\rm GHz}^{1/2}. \tag{11}$$

The synchrotron power emitted by such electrons is

$$P_{\rm synch} \approx 3.8 \times 10^{-18} \left(\frac{B}{0.06\ \text{G}}\right)^2 \gamma_e^2\ \text{erg s}^{-1}$$
$$\approx 1.6 \times 10^{-14} \left(\frac{B}{0.06\ \text{G}}\right) \nu_{\rm GHz}\ \text{erg s}^{-1}. \tag{12}$$

The synchrotron cooling time is then

$$t_{\rm cool} = \frac{\gamma_e\, m_e c^2}{P_{\rm synch}} \approx 6800 \left(\frac{B}{0.06\ \text{G}}\right)^{-2} \gamma_e^{-1}\ \text{yr}$$
$$\approx 105 \left(\frac{B}{0.06\ \text{G}}\right)^{-3/2} \nu_{\rm GHz}^{-1/2}\ \text{yr}. \tag{13}$$

The cooling time is substantially longer than the duration of the encounter for any value of the Lorentz factor γ_e or, equivalently, any frequency $\nu_{\rm GHz}$ of interest for radio or submillimeter observations. Thus, all the shocked electrons will contribute to the observed synchrotron emission.

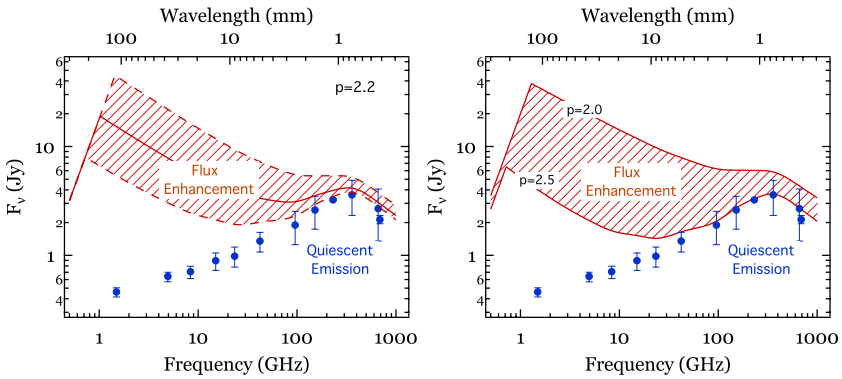

Figure 3. Radio emission expected from non-thermal electrons accelerated in the bow shock of G2, plotted along with the quiescent emission observed from Sgr A*. The data points are compiled from Falcke et al. (1998), Zhao et al. (2003), and Marrone et al. (2008). The solid line in the left panel shows the predicted spectrum for our fiducial model with power-law index $p = 2.2$ (Equation (9)). The hatched area bounded by dashed lines corresponds to a factor of three uncertainty each way in the number of accelerated electrons, i.e., the acceleration efficiency is varied from 1.7% to 15%. The hatched region in the right panel shows the predicted radio flux for power-law indices in the range $p = 2$–2.5, keeping the fraction of accelerated electrons fixed at 5%. In both panels, the turnover of the flux at low frequencies is caused by synchrotron self-absorption.

(A color version of this figure is available in the online journal.)

To estimate the expected spectral flux from the shocked electrons, we use the electron Lorentz factor distribution given in Equation (9) and assume a distance $D = 8.3$ kpc to the Galactic center. Then, using the standard formula for synchrotron emission from a power-law distribution of electrons (Rybicki & Lightman 1979), we obtain

$$F_\nu \approx 19 \left(\frac{B}{0.06\ \mathrm{G}}\right)^{1.6} \nu_{\mathrm{GHz}}^{-0.6}\ \mathrm{Jy}, \quad p = 2.2. \tag{14}$$

This estimate is valid over the range of frequencies at which the synchrotron emission is optically thin. The predicted flux is fairly large and should be easily detected over a wide range of radio frequencies, provided particle acceleration in the bow shock is as efficient as the numerical simulations described in Section 3 indicate.

At low frequencies, the synchrotron emission will be self-absorbed. Using standard results (Rybicki & Lightman 1979), we estimate the source function of the shocked electrons to be

$$S_\nu = 3.7 \times 10^{-8} \left(\frac{B}{0.06\ \mathrm{G}}\right)^{-1/2} \nu_{\mathrm{GHz}}^{5/2}\ \mathrm{erg\ cm^{-2}\ s^{-1}\ Hz^{-1}\ sr^{-1}}. \tag{15}$$

Assuming a circular source of radius 10^{15} cm at distance D, the limiting synchrotron flux due to self-absorption is

$$F_{\nu,\mathrm{max}} \approx 18 \left(\frac{B}{0.06\ \mathrm{G}}\right)^{-1/2} \nu_{\mathrm{GHz}}^{5/2}\ \mathrm{Jy}. \tag{16}$$

The quiescent emission from Sgr A* is well below this level at frequencies above a GHz, so self-absorption should not interfere with our ability to observe the additional emission.

In Figure 3, we show the predicted radio emission from shock-accelerated electrons in the bow shock of G2. In order to account for potential uncertainties in our estimates of shock parameters (Section 2) and our simulations of particle acceleration (Section 3), we explore the dependence of the expected flux enhancement on (left panel) the number of accelerated electrons and (right panel) the power-law index of the electron energy distribution. We also show in Figure 3 the measured quiescent flux at different frequencies, with the error bars indicating the degree of variability among different observations. At 1.4 GHz, the quiescent radio flux of Sgr A* is 0.5 Jy, whereas we estimate that the flux enhancement could be as large as 10 Jy. The additional synchrotron emission ought to be easily detectable at GHz frequencies. Note also that the spectral index is predicted to change substantially.

5. DISCUSSION

The passage of the recently discovered cloud of gas, G2, near Sgr A* presents a unique opportunity to study the dynamics and properties of hot gas in the vicinity of the black hole at the Galactic center. In this Letter, we showed that a bow shock may form during the pericentric passage of the cloud, and we investigated the flux enhancement in the 1–100 GHz frequency range that will arise as a result of particle acceleration in the shock front. We ran first-principles PIC simulations for shock parameters appropriate to the bow shock and thereby obtained realistic estimates of the energy distribution of accelerated electrons. Using these results, we calculated the likely synchrotron emission from the bow shock and found that the additional flux might exceed the quiescent emission from Sgr A* by up to an order of magnitude at GHz frequencies. This suggests that there is a good chance of detecting enhanced radio emission as G2 plows through the ambient hot medium around the time of pericentric passage. Since the cooling time of the accelerated electrons is estimated to be long, the enhanced emission should continue well after the encounter.

There are order unity uncertainties in the parameters we have assumed for the bow shock, and hence the predictions made in this Letter are not likely to be quantitatively accurate. We have allowed for some of these uncertainties while computing the hatched regions shown in the two panels in Figure 3. An additional uncertainty is whether or not a bow shock will form in the first place. Gillessen et al. (2012) discuss a compression shock moving into the cloud, which will inevitably be accompanied by an external shock moving into the ambient medium, the bow shock in our model. In most models of G2 (Burkert et al. 2012; Miralda-Escude 2012; Schartmann et al. 2012; Murray-Clay & Loeb 2012), the cloud retains some level of integrity during its pericentric passage and thus is likely to develop an external shock. However, if the cloud is completely shredded by Kelvin–Helmholtz or other instabilities before a

bow shock forms, then our synchrotron emission estimates will no longer be valid.

Given the pericentric distance of 3100 R_S, which corresponds to a projected angle of ∼33 mas, the bow shock emission should be displaced from the quiescent radio emission of Sgr A* by the same amount. At wavelengths $\lesssim$6 cm, this angular distance is larger than the size of the scattering ellipse of Sgr A* (Bower et al. 2006) and ought to be resolved by interferometric observations. The scatter-broadening of the radio image of Sgr A* is believed to be caused by a compact foreground interstellar cloud that is at least ∼100 pc from the black hole (Frail et al. 1994). Thus, the broadening is unlikely to be affected by any gas stripped from G2 during its pericentric encounter.

In addition to the bow shock and the associated prompt radio synchrotron emission considered in this Letter, it is expected that the cloud G2 will also shed mass as it interacts with the ambient hot gas. A likely early signature of the increase in the gas density at a few thousand R_S is a change in the observed Faraday rotation above a GHz, which may provide the first estimates of the increase in the mass accretion rate. As it moves inward, this gas will cause the mass accretion rate onto the central black hole to be enhanced over a period of many years. Such an increase could cause a secular change in the radio flux of Sgr A* on a timescale of ten years to several decades, accompanied by changes in the "silhouette" of the black hole that could be monitored by future interferometers (Moscibrodzka et al. 2012).

R.N. thanks A. Loeb and N. Stone for useful discussions and L.S. thanks A. Spitkovsky for insightful comments. R.N. gratefully acknowledges support from NASA grant NNX11AE16G, and F.Ö. from NSF grant AST-1108753. L.S. is supported by NASA through Einstein Postdoctoral Fellowship grant No. PF1-120090 awarded by the Chandra X-ray Center, which is operated by the Smithsonian Astrophysical Observatory for NASA under contract NAS8-03060. The simulations were performed on the Odyssey cluster at Harvard University, on the PICSciE-OIT High Performance Computing Center and Visualization Laboratory at Princeton University, and on TeraGrid resources under contract No. TG-AST120010.

REFERENCES

Begelman, M. C., & Kirk, J. G. 1990, ApJ, 353, 66
Blandford, R., & Eichler, D. 1987, Phys. Rep., 154, 1
Bower, G. C., Goss, W. M., Falcke, H., Backer, D. C., & Lithwick, Y. 2006, ApJ, 648, L127
Burkert, A., Schartmann, M., Alig, C., et al. 2012, ApJ, 750, 58
Falcke, H. 1999, in ASP Conf. Ser. 186, The Central Parsecs of the Galaxy, ed. H. Falcke, A. Cotera, W. J. Duschl, F. Melia, & M. J. Rieke (San Francisco, CA: ASP), 113
Falcke, H., Goss, W. M., Matsuo, H., et al. 1998, ApJ, 499, 731
Falcke, H., & Markoff, S. 2000, A&A, 362, 113
Frail, D. A., Diamond, P. J., Cordes, J. M., & van Langevelde, H. J. 1994, ApJ, 427, L43
Ghez, A. M., Salim, S., Weinberg, N. N., et al. 2008, ApJ, 689, 1044
Gillessen, S., Eisenhauer, F., Trippe, S., et al. 2009, ApJ, 692, 1075
Gillessen, S., Genzel, R., Fritz, T. K., et al. 2012, Nature, 481, 51
Macquart, J.-P., & Bower, G. C. 2006, ApJ, 641, 302
Marrone, D. P., Baganoff, F. K., Morris, M. R., et al. 2008, ApJ, 682, 373
Matsukiyo, S., Ohira, Y., Yamazaki, R., & Umeda, T. 2011, ApJ, 742, 47
Medvedev, M. V., & Loeb, A. 1999, ApJ, 526, 697
Miralda-Escude, J. 2012, ApJ, 756, 86
Moscibrodzka, M., Shiokawa, H., Gammie, C. F., & Dolence, J. C. 2012, ApJ, 752, L1
Murray-Clay, R. A., & Loeb, A. 2012, arXiv:1112.4822
Narayan, R., & Yi, I. 1994, ApJ, 428, L13
Narayan, R., Yi, I., & Mahadevan, R. 1995, Nature, 374, 623
Özel, F., Psaltis, D., & Narayan, R. 2000, ApJ, 541, 234
Riquelme, M. A., & Spitkovsky, A. 2011, ApJ, 733, 63
Rybicki, G. B., & Lightman, A. P. 1979, Radiative Processes in Astrophysics (New York: Wiley)
Schartmann, M., Burkert, A., Alig, C., et al. 2012, ApJ, 755, 155
Spitkovsky, A. 2005, in AIP Conf. Ser. 801, Astrophysical Sources of High Energy Particles and Radiation, ed. T. Bulik, B. Rudak, & G. Madejski (Melville, NY: AIP), 345
Weibel, E. S. 1959, Phys. Rev. Lett., 2, 83
Xu, Y.-D., Narayan, R., Quataert, E., Yuan, F., & Baganoff, F. K. 2006, ApJ, 640, 319
Yuan, F., Quataert, E., & Narayan, R. 2003, ApJ, 598, 301
Zhao, J., Ekers, R. D., Goss, W. M., Lo, K. Y., & Narayan, R. 1989, in IAU Symp. 136, The Center of the Galaxy, ed. M. Morris (Dordrecht: Kluwer), 535
Zhao, J.-H., Young, K. H., Herrnstein, R. M., et al. 2003, ApJ, 586, L29